Electrostatic Nanoassembly of Novel Composites

Subjects: Others

Contributor: Hiroyuki Muto , Atsushi Yokoi , Wai Kian Tan

Electrostatic assembly is one of the bottom–up approaches used for multiscale composite fabrication. Since its discovery, this method has been actively used in molecular bioscience as well as materials design and fabrication for various applications. Despite the recent advances and controlled assembly reported using electrostatic interaction, the method still possesses vast potentials for various materials design and fabrication. This review article is a timely revisit of the electrostatic assembly method with a brief introduction of the method followed by surveys of recent advances and applications of the composites fabricated. Emphasis is also given to the significant potential of this method for advanced materials and composite fabrication in line with sustainable development goals. Prospective outlook and future developments for micro-/nanocomposite materials fabrication for emerging applications such as energy-related fields and additive manufacturing are also mentioned.

electrostatic assembly   polyelectrolytes   composites   ceramics   polymers

additive manufacturing

1. Introduction

Nanomaterials exhibit unique properties that are not seen in bulk materials, and this has led to an increase in the development of nanocomposites for various applications. In composite materials design and fabrication, the approach used is either a top–down or bottom–up approach [1][2]. However, the bottom–up approach offers better flexibility in terms of dimension control, shape ability, and surface-charge modification to achieve desired properties and functionalities [3]. An example of a bottom–up approach in materials design is the electrostatic assembly (EA) method. Caruso first reported the formation of multilayer silica nanoparticles on polystyrene latex using the EA method in 1998 [4]. Since then, the EA method has been widely used for the design and fabrication of materials such as bio-components [5][6][7], polymers [8][9], inorganic materials [10], and carbon-based materials such as graphene and fullerene [11][12].

In this review, a brief overview of an electrostatic assembly is first described, followed by a comprehensive survey of the current progress in composite materials design via the EA method as well as its prospective outlook for future development. Emphasis on emerging applications using EA assembly is given in this review.

1.1. The EA Method

In earlier days, the EA method involved the use of the Langmuir–Boldgett (LB) technique where monolayers generated on water were transported onto a solid supporting structure. With the limitations in equipment, substrate size, as well as film quality of the LB technique, the self-assembly of films using covalent and coordination chemistry was developed. However, this technique was only applicable for certain classes of organic materials with limited design flexibility, and a high-quality multilayered structure cannot be achieved. To achieve a good nano-architectured film yield regardless of the substrate topology and nature, a suitable alternative is to employ the electrostatic attraction of molecules with opposite charges as a driving motion for the multilayer and nanoarchitecture build up [13]. Decher et al. first reported the formation of one or multiple layered composite films (coatings) via a layer-by-layer (LbL) adsorption of polyelectrolytes in aqueous solution. The basic principle of this technique involves the repulsion of equally charged molecules (induced using polyelectrolytes) as well as the attraction and adsorption of oppositely charged molecules to the initial molecule leading to form well controlled multilayer structured films after several cycles [14].

Subsequently, many studies have been reported using the EA method and LbL assembly for various applications. The reason for this boom is the feasibility of using the EA method for controlled decoration of desired additives at the nano and micro levels irrespective of the object's shape and dimensions, which is not achievable using conventional mixing methods . The attractive features of this approach include the controllability of additive coverage percentage on a primary particle and controllability of multiple-component layered films formation with good precision [15]. Studies focusing on biomaterials and biomedicine for drug delivery and cell cultivation have been reported [16][17][18]. As the awareness for achieving the sustainability development goals (SDGs) began to grow in our daily lives, the development of materials for sustainable-related technologies such as renewable energies (fuel cells, solar cells), water treatment, efficient energy storage systems (batteries and capacitors), and additive manufacturing have been deemed as emerging technologies and taken the center stage in research and development. Low environmental load processes have been recognized as a way of achieving SDGs through efficient energy usage and the effective utilization of natural resources without leaving heavy footprints on the environment. Given that the EA method is a green process approach, it is expected to play an important role in materials design to achieve the SDGs.

2. Composite Fabrication via EA Method and their Applications

2.1. Formation of Electromechanical or Electrochromic Responsive LbL Composite Films

Using the EA method in the formation of LbL films, the controlled deposition of films can be achieved. By utilizing the LbL assembled films as a building block, further optimization and coupling via electrochemical methods can be used to fabricate functional nano-devices such as sensors, microelectromechanical systems (MEMS), and electrochromic materials. The strategy is to incorporate electro-responsive materials within the LbL films in the generation of stimuli responsive polymer composite films. For example, in the development of MEMS systems, a transducer that converts electrical energy to mechanical energy is one of the core components. In the development

of low-cost MEMS, many researchers are focusing on the development of electroactive polymers because they are inexpensive, possess a wide range of environmental endurance, and have good compatibility with many fabrication techniques. To incorporate redox active materials in the fabrication of electro-responsive materials, electro-swelling/deswelling of LbL films is commonly used. Hence, the assembled LbL films will experience swelling/deswelling during ion exchange due to the redox of the incorporated active materials. The electroactive materials confined or embedded within the electrostatic deposited film exhibited improved electro-responsive properties. One example of the above-mentioned phenomenon is shown in Figure 1, where the redox of ferrocyanide ions within the electrostatic assembled films of polyglutamic acid and poly (allylamine hydrochloride) resulted in the electro-swelling of the LbL assembled films. During charge compensation, the diffusion of counter-anions with water molecules occurs causing the swelling and deswelling process, which can be controlled by changing the salts dissolved in the solution.
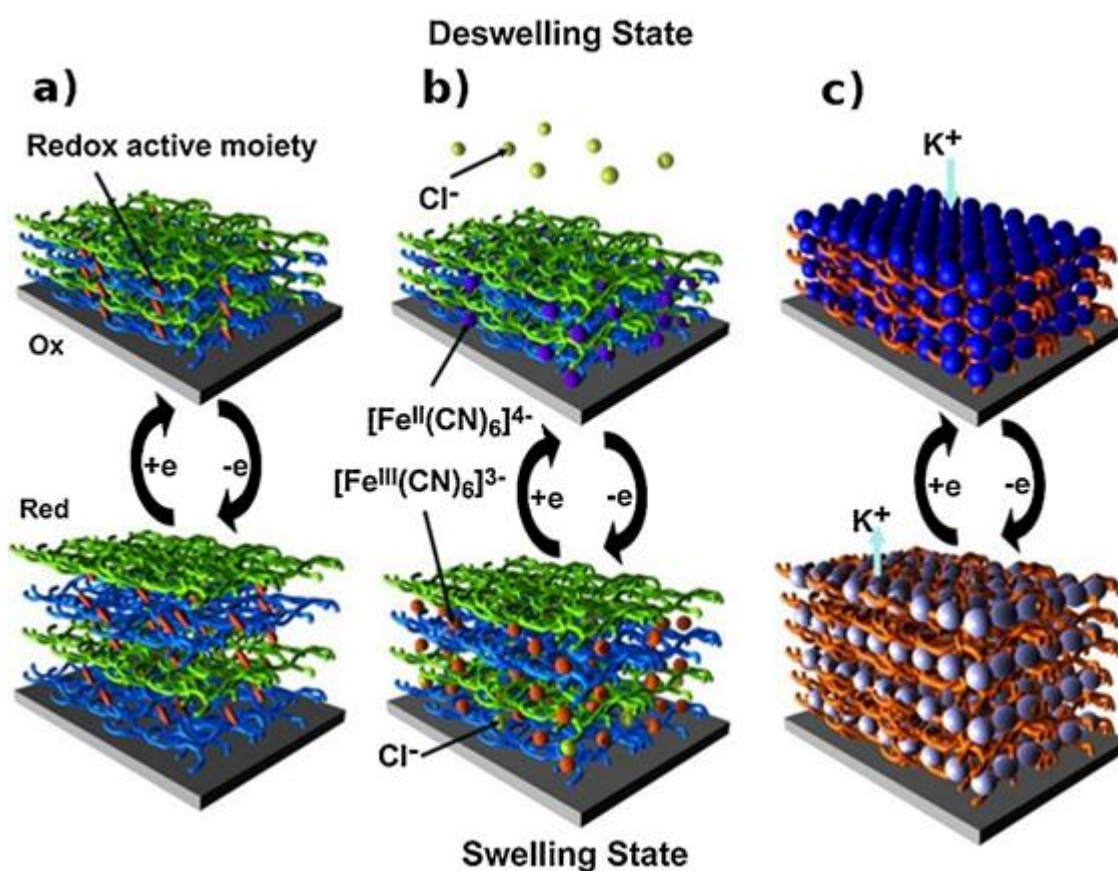

Figure 1. Electro-swelling processes of LbL films. Electro-swelling/deswelling of LbL films based on (**a**) redox active moieties grafted onto one of the polyelectrolytes, (**b**) free redox active molecules confined in LbL films, and (**c**) redox active component-based film. Reprinted with permission from [15], copyright (2015) Elsevier.

In a recent study on the fabrication of a flexible electrochromic display, Qi et al. demonstrated the formation of 2D composite materials consisting of V_2O_5 nanosheets and graphene films using the electrostatic LbL method, as shown in Figure 2a. The composites exhibited an impressive ultrafast response time in coloring and bleaching because of the reduced agglomeration, improved electronic conductivity, and reduced charge transport distance, as shown in Figure 2b [19]. When the endurance of the device was tested by bending at an angle of 90° for 100

cycles, rapid electrochromic response time was still observed. This shows that the EA method possesses excellent potential for the future development of flexible devices.
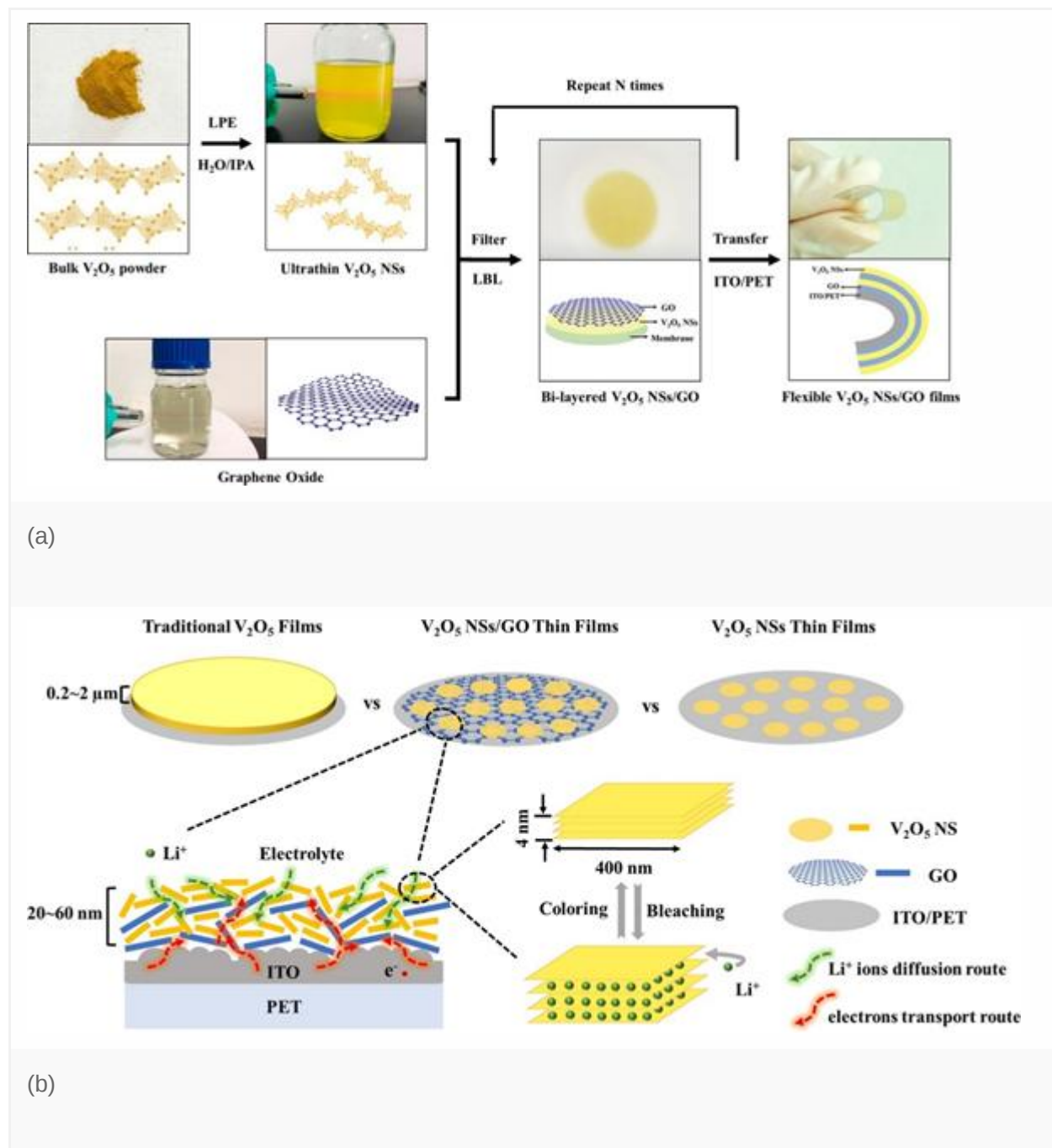

(a)

(b)

Figure 2. (**a**) Schematic illustration of the LbL assembly process of flexible V_2O_5 NSs/GO@ITO/PET films. (**b**) Schematic illustration of the coloring and bleaching processes of V_2O_5 NSs/GO films. Reprinted with permission from [19], copyright (2020) Elsevier.

2.2. Composite LbL Films for Biomedicine and Biomimetic Extracellular Matrix

In the early stage of LbL development, most studies focused on the use of synthetic polyelectrolytes. However, when considering the application of EA and LbL techniques for biomedical and biomaterials applications, researchers began to focus on the use of natural polyelectrolytes such as chitosan, dextran, amine hyaluronic acid, heparin, etc. . The use of natural polyelectrolytes in LbL assembly provides a new potential for the development of advance structural composites with precise design such as core–shells for drug delivery. Furthermore, the flexibility of post-treatment after LbL assembly is an added advantage, especially for altering the physicochemical properties of the assembled composite films. Parameters such as temperature, light irradiation, electric field induction, pH adjustment, and vibrational stimulation can be used to adjust the properties.

For the functionalization of biomaterials, it is important to create a microenvironment that mimics the extracellular matrix . By designing polymeric LbL films, current progress has enabled the development from only mimicking cell configuration to the possible control of cell behaviors . The possibilities of biochemical engineering via the EA method is vital for the advancement in biomaterials and tissue engineering fields . Due to the good stability of electrostatically assembled films in aqueous solution and its dynamic potential, the microenvironment generated, which is almost equivalent to the natural cellular matrix, is crucial due to the cells' selective recognition to certain biochemical and biophysical conditions. Liu et al. have demonstrated protein immobilization through matrix binding via the LbL technique. As shown in the schematic in Figure 3, the immobilization of a chemoattractant known for hematopoietic stem cell homing and cancer progression called stromal cell-derived factor-1 (SDF-1α) was achieved using poly(l-lysine) (PLL) and hyaluronan (HA) polyelectrolytes using the LbL process. This resulted in a significant increase in human epithelial breast cancer cell spreading in the matrix-bound SDF-1α. From their investigation, they found that the cell adhesion on films with matrix-bound SDF-1α exhibited an obvious spatial organization with good focal adhesion compared to the cells presented with a soluble cue [20]. Their study showed that LbL films were effective as a biomimetic tumoral niche in revealing potent cellular effects as well as underlying mechanisms that can be useful for the research in regenerative therapies against cancer cells such as breast cancer.
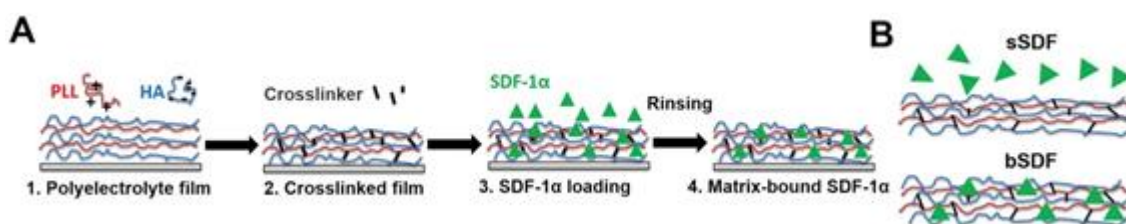

Figure 3. (**A**) Successive steps for the preparation of matrix-bound stromal cell-derived factor-1 (SDF-1α) using layer-by-layer films as extra-cellular matrix with poly(l-lysine) (PLL) and hyaluronan (HA) as polyelectrolytes. The film is first deposited step-by-step (1), then cross-linked (2) and finally loaded with SDF-1α in acidic conditions (1 mM HCl) (3), followed by a rinsing step in order to obtain matrix-bound SDF-1α (4). (**B**) SDF-1α can be presented as a soluble cue (sSDF) or in a matrix-bound manner (bSDF). Reprinted with permission from [20], copyright (2017) Elsevier.

2.3. Composite Materials for Energy Storage and Conversion Technologies

Recent development in the Internet of Things and electric vehicles has resulted in a demand surge for composite materials with high storage and energy capacity. Electrochemical energy storage systems such as lithium-ion batteries, lithium-sulfur, and metal–air batteries have attracted attention due to their high specific energy capacity [21][22]. In a recent study carried out on all-solid-state lithium–sulfur batteries, Phuc et al. reported the use of the EA method in the design of their solid electrolyte consisting of 0.67 Li_3PS_4–0.33 LiI (LPSI) and sulfur–carbon nanofiber (S-CNF) using a novel liquid phase route [23]. The schematic for the preparation of the S-CNF via the EA method is shown in Figure 4a–c, while Figure 4d shows the SEM image and energy-dispersive X-ray (EDX) mapping of the S-CNF–LPSI composite. The proper distribution of S-CNF within the LPSI promoted an electrically conductive pathway to overcome the Li_xS_y electronic insulation behavior, enabling a good lithium–sulfur battery performance. In the development of Fe–air batteries, Tan et al. reported a facile and simple way to decorate iron oxide particles (Fe_3O_4) at room temperature on carbon paper in a short period of 10 min using the EA method. The Fe_3O_4-decorated carbon paper was used in the evaluation of alkaline aqueous and all-solid-state Fe-air batteries with a maximum discharge capacity of 460 and 70 mAh g^{-1}, respectively [24].
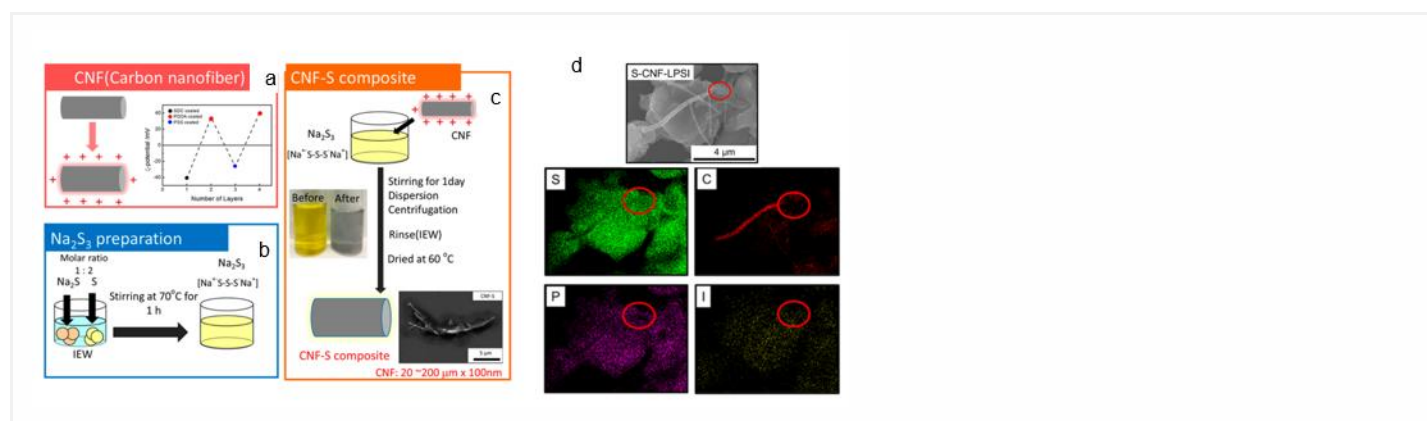

Figure 4. Schematics of sulfur–carbon nanofiber (S-CNF) composite preparation: (**a**) adjustment of the CNF surface charge, (**b**) formation of Na_2S_3 solution, (**c**) S-CNF composite formation. The SEM image and and energy-dispersive X-ray (EDX) mapping results for S, C, P, and I of the S-CNF−LPSI (Li_3PS_4–0.33 LiI) composite are shown in (**d**). Reprinted with permission from [23], copyright (2020) ACS.

As 2D graphene-derived materials are becoming an integral part of the materials used in the development of advanced functional composites, they have been incorporated in various composites for a wide range of applications . The application of the EA method for the integration of graphene materials into composites has been reported in the literature. For supercapacitor applications, Fenoy et al. reported on the fabrication of electrode materials using electrostatic assembled polyaniline–PSS complex layer with iron oxide nanoparticles decorated graphene layers in aqueous solution [11]. They demonstrated an excellent electrochemical capacitance of 768.6 and 659.2 F g^{-1} in 0.1M HCl and 0.1M KCl (at 1A g^{-1}), respectively with high cycling stability up to 1600 cycles. In another interesting development, a possible diffusion-driven mechanism of LbL assembled layers was reported by Hong et al. They demonstrated the formation of a porous reduced graphene oxide (rGO)/polyaniline (PANI) composite as the binder-less electrode for supercapacitors [25]. The strong electrostatic interaction between graphene oxide (GO) and the branched polyethyleneimine after the diffusion process enabled the formation of a

porous foam-like structure as a template for the polymerization of PANI, as shown in Figure 5. This simple fabrication of a binder-less electrode yielded a capacitance performance of 438.8 F g^{-1} at 0.5 A g^{-1} in 1 M H$_2$SO$_4$.
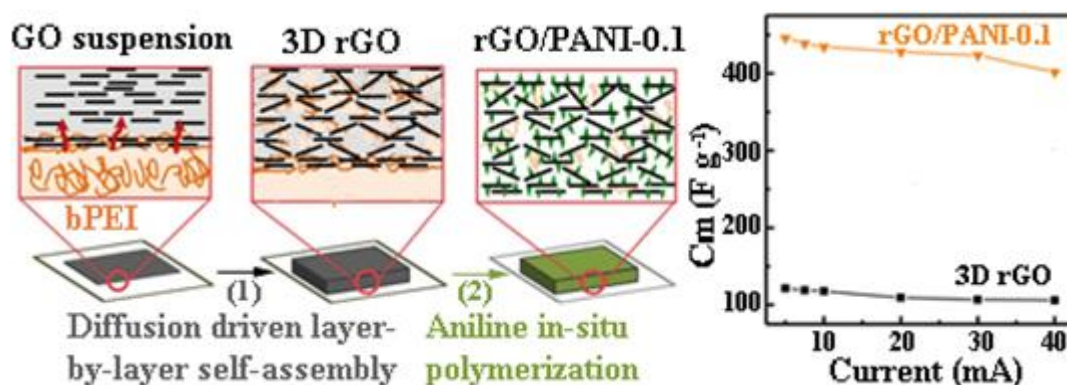

Figure 5. Schematics of preparing reduced graphene oxide (rGO)/PANI (polyaniline) composite film. Branched polyethyleneimine (bPEI) solution was coated on a filter paper. The coated paper was immersed in assembly graphene oxide (GO) suspension. GO and bPEI formed a stable complex layer at first. Then, bPEI diffused out of the reservoir and complexed with GO sheets. This complexation and diffusion process continued, eventually developing into a thicker GO/bPEI composite film. Some square GO/bPEI films (2 × 2 cm^2) were cut and detached from the substrate, then subjected to a hydrothermal treatment at 190 °C. Finally, the hydrothermally reduced-GO films were used as a template for the polymerization of aniline. The rGO/PANI exhibits capacitance of 438.8 F g^{-1} at 0.5 A g^{-1} in 1 M H$_2$SO$_4$. Reprinted with permission from [25], copyright (2017) Elsevier.

For fuel cell applications, proton exchange membrane fuel cell (PEMFC), which possesses a high energy conversion efficiency and low-cost fabrication, is an alternative source for a clean energy [26]. Currently, researchers are working on the development of PEMFC due to its higher reaction kinetics and easier heat management. Current challenges include obtaining a polyelectrolyte membrane (PEM) that exhibits good proton conduction at elevated temperature and low humidity [27]. In order to obtain a higher phosphoric acid uptake to promote higher proton conductivity, the formation of organic–inorganic hybrid membranes to improve the physico- and electrochemical properties of the PEM were reported [28][29][30]. Using the EA assembly, controlled multilayer LbL membrane formation enabled the fabrication of PEM with desired properties such as improved proton conductivity and mechanical property [31]. Che et al. reported the formation of multilayer-component PEM using sulfonated polyetheretherketone (SPEEK) as a polyanion while polyurethane (PU) and the ionic liquid of 1-butyl-3-methylimidazolium were used as a polycation, as shown in Figure 6. The films obtained as shown in Figure 6 had a thickness of approximately 25 μm after 100 layers of coating, and the films exhibited satisfactory mechanical strength and excellent conductivities with different phosphoric acid doping levels [27].
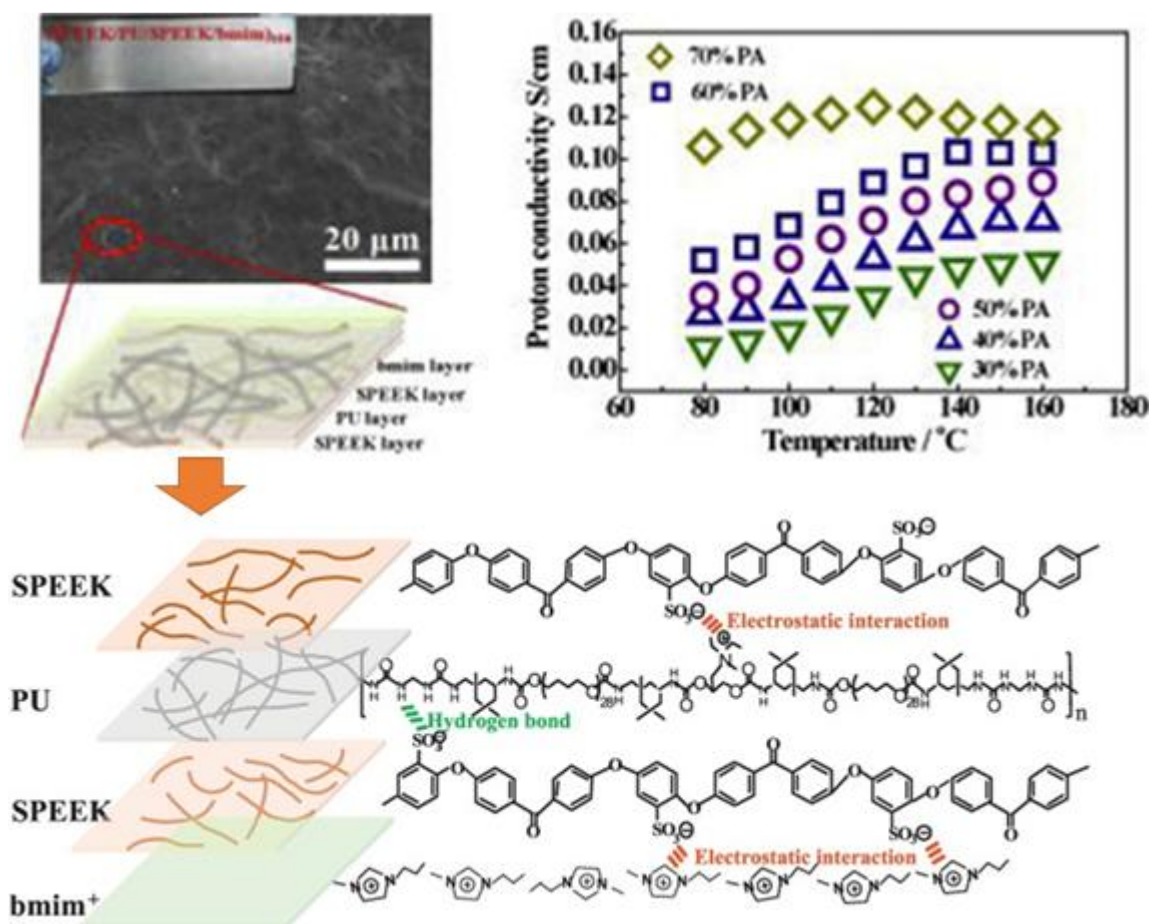
Figure 6. Multi-component membrane of SPEEK–PU–SPEEk–bmim obtained via the LbL method, which demonstrated a maximum proton conductivity of 1.03×10^{-1} S/cm. Schematic of the interaction force between SPEEK and PU, SPEEK and bmim^{+} in one layer of the LbL membrane. Reprinted with permission from [45], copyright (2019) Elsevier. PU: polyurethane, SPEEK: sulfonated polyetheretherketone, bmim: 1-butyl-3-methylimidazolium.

2.4. Composite Materials for Additive Manufacturing

Additive manufacturing (AM) technology is regarded as the next-generation manufacturing revolution that would enable the rapid and moldless formation of complicated components [32][33][34][35][36]. The potential of AM is massive for the production of functional composites from a wide range of materials such as metals, polymers, and ceramics. AM enables the rapid prototyping and transformation of product manufacturing with precise customization. The synchronization of computer–aided design with AM has enabled the formation of complex 3D structures within a short time with maximum material utilization while enabling flexible customization and design. According to Tofail et al., AM is close to being a "bottom–up" manufacturing process, where the desired structure is fabricated using a "layer-by-layer" approach, resulting in unprecedented freedom in the manufacturing processes [34]. In AM 3D printing technology, the ability to sinter the materials via indirect and direct laser sintering of the printed artifact is one important factor for rapid prototyping. Although breakthroughs have been reported for metal and polymeric materials, laser sintering of ceramics remains a challenge due to their high melting point, poor thermal shock resistance, poor ductility, and limited laser absorptivity [37][38]. In the work reported by Kuwana et al., cellulose

nanofiber (CNF) decorated alumina (Al_2O_3) powders obtained via EA were used as a composite for the selective laser sintering of Al_2O_3. The EA method enabled the homogeneous adsorption of CNF onto Al_2O_3 particles, which were converted to carbon residue after the heat treatment to allow improved laser absorption for the sintering process. The feasibility of using naturally abundant CNF in materials design also promotes sustainability for AM. In another recent work, Yavari et al. studied additive manufactured bio-functionalized meta-biomaterial composites with infection prevention and bone tissue regenerative properties [39]. The LbL coating was carried out using gelatin- and chitosan-based coatings containing either bone morphogenetic protein (BMP)-2 or vancomycin on the surface of selective laser melted porous structures made from commercial pure titanium, as shown in Figure 7. This study unequivocally demonstrates that multifunctional additive manufactured composite materials can be fabricated using the EA method.
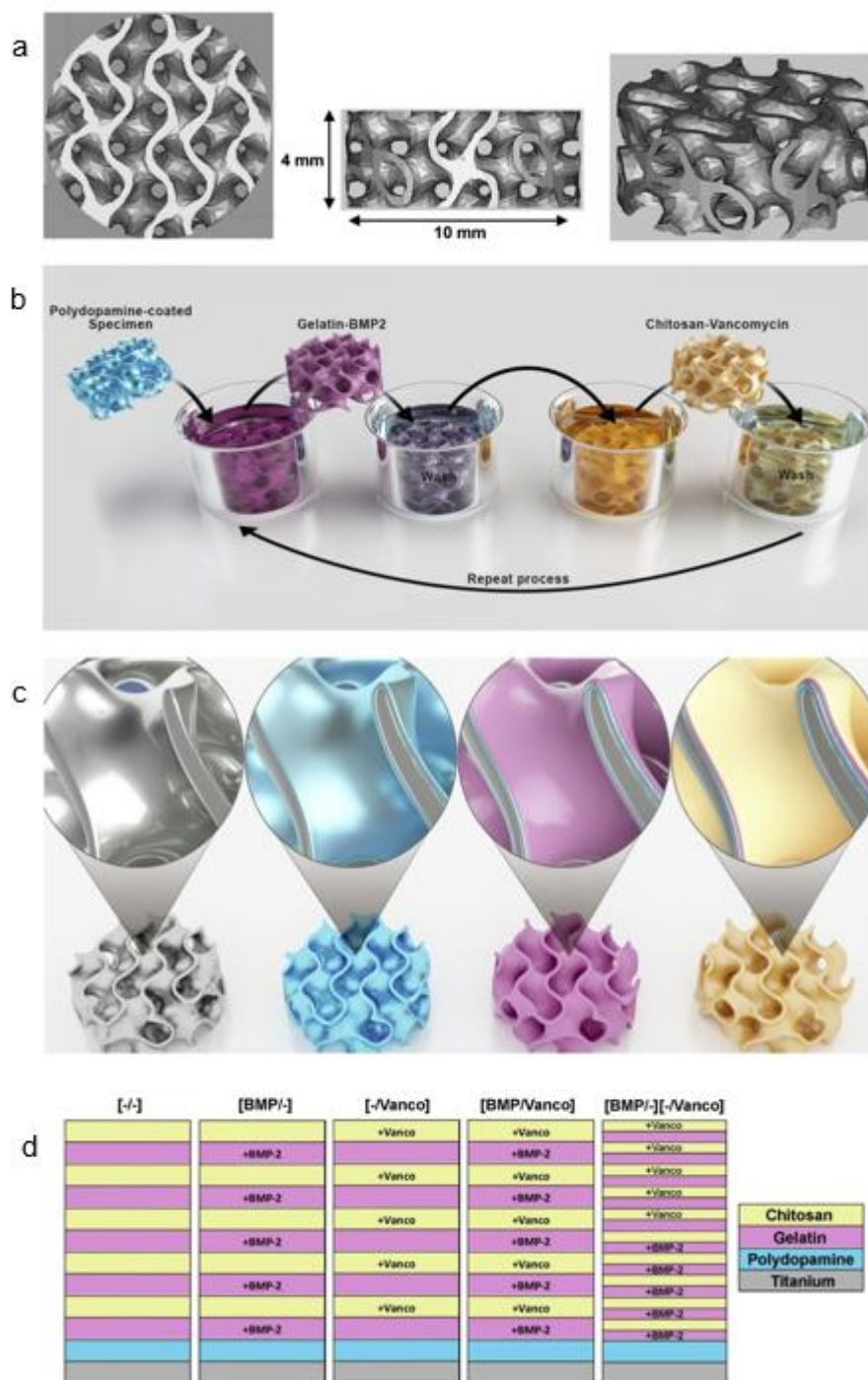
Figure 7. Computer-aided design drawings of the porous structured titanium used as input for the AM process (**a**). Schematic illustration of the layer-by-layer coating process (**b**,**c**) and the resulting surface layers (**d**). Reprinted with permission from [39], copyright (2020) Elsevier.

2.5. Ceramic Composites

2.5.1. Mechanical Properties Control of Carbon-Based Al_2O_3 Composites

Carbon-based Al_2O_3 composites have attracted attention due to their exceptional mechanical properties such as failure strength, toughness, and wear resistance [40]. In addition, other properties such as the electrical and thermal properties of these composites can also be altered [41][42][43]. By using the EA method to control the decoration of carbon additives on Al_2O_3, the mechanical properties of carbon–ceramic composites can be achieved. In a recent study that used microparticles of Al_2O_3 granules with adsorbed carbon nanoparticles (CNP) on their surface, Tan et al. demonstrated that by controlling the amount of CNP additives and Al_2O_3 microparticle size, different surface coverage could be obtained. This led to a controlled microstructure formation with controllable mechanical properties. The good homogeneity of CNP decorated on Al_2O_3 particles played an important role in the formation of an interconnected carbon layer along the Al_2O_3 boundaries influencing the final mechanical properties, as shown in Figure 8 . The controlled amount of CNP decoration at the grain boundaries influenced the hardness of the composites, which was determined by an indentation test.
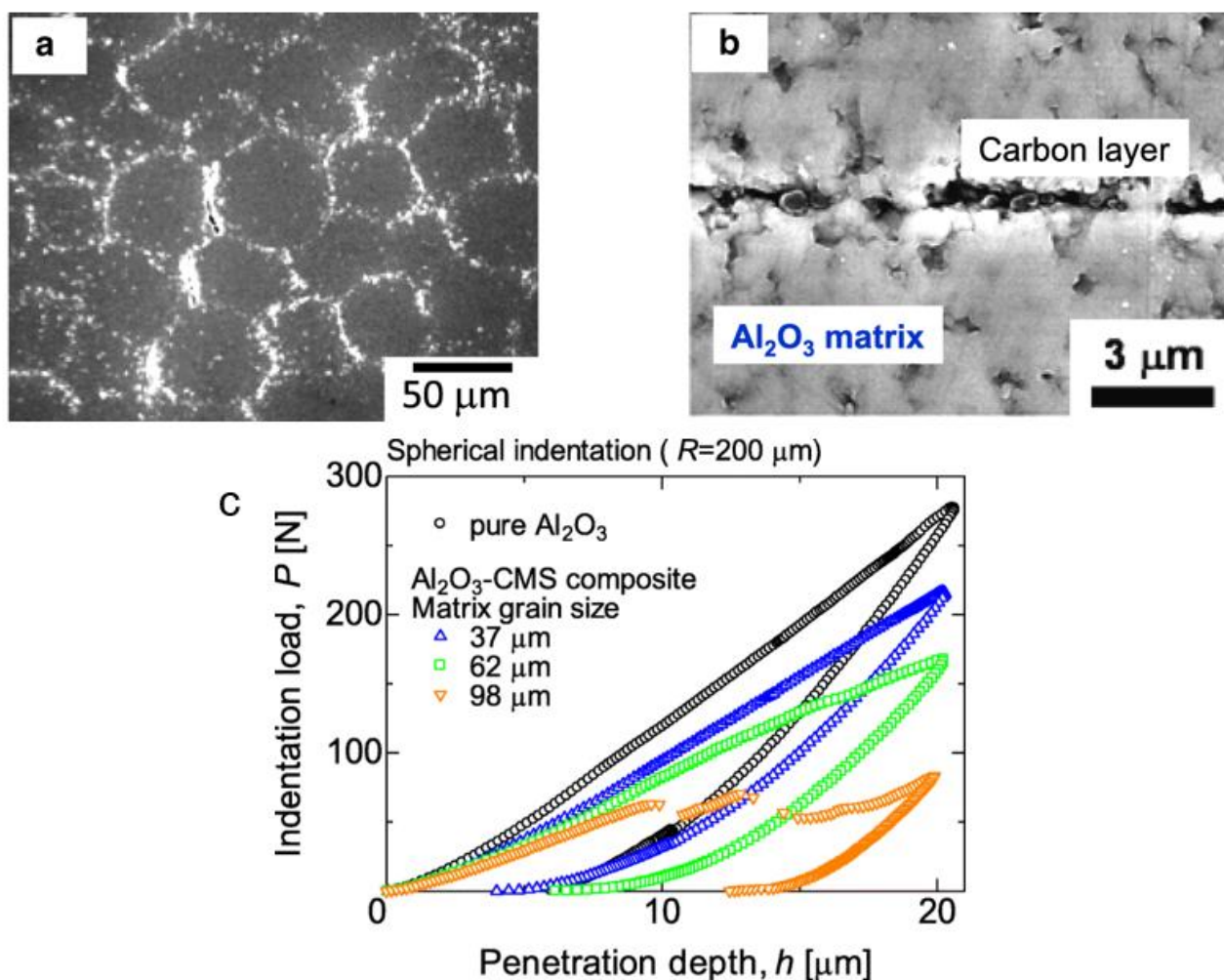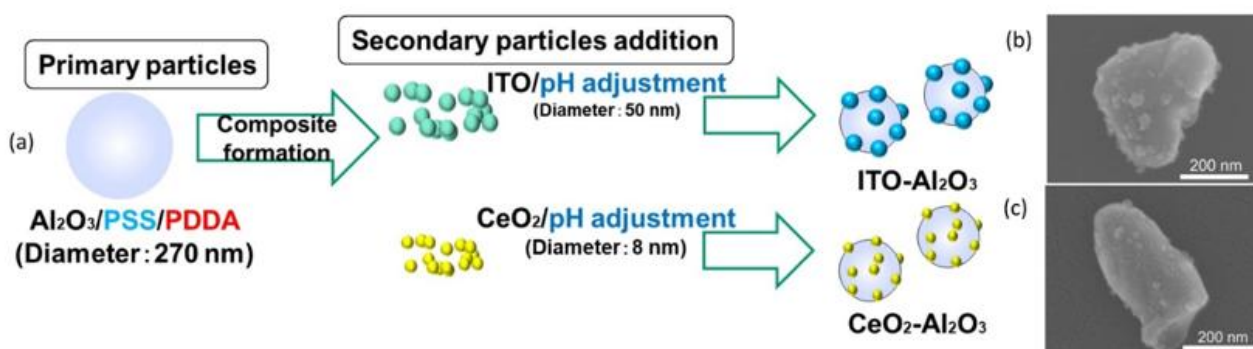

Figure 8. (**a**) Microstructure of 0.6 vol% carbon nanoparticles (CNP)–Al_2O_3 composite using Al_2O_3 with the average diameter of 62 μm. (**b**) Grain boundary of CNP–Al_2O_3 composite. A carbon layer could be observed at the interface between the Al_2O_3 matrix. (**c**) Hysteresis curves of indentation load and penetration depth of 1.0 vol% CNP–Al_2O_3 composites.

2.5.2. Porous Ceramic Composites

Porous ceramic materials with controllable microstructures possess a good potential for applications such as heat insulation, sound dampening, bio-ceramics, and as catalyst carriers for lightweight structural components [44][45]. In the fabrication of porous ceramic materials, various methods such as sol–gel, freeze-casting, the addition of a pore-forming agent, and partial sintering methods are employed [46][47]. However, the achievement of a controlled homogenous distribution of the porous structure remains a challenge, especially when more than one elemental material is used in the composite mixture. The use of the EA method to control the formation of a porous ceramic material consisting of Al_2O_3 and silica (SiO_2) without the use of pore-forming agents has been recently reported. By changing the volume percent of SiO_2 particles addition, which affects the coverage percentage of SiO_2 on the surface of Al_2O_3, the control of microstructure formation, open porosity, as well as the mechanical properties of the sintered Al_2O_3–SiO_2 composite ceramics were demonstrated.

2.5.3. Translucent Ceramic Composite Films with Controllable Optical Properties

In ceramic film formation, thermal spraying and chemical vapor deposition are commonly used. Due to limitations such as expensive equipment and the thermal stability of substrates, researchers have opted for a more rapid and low-temperature ceramic film fabrication method [48][49]. The feasible formation of compact ceramic films by aerosol deposition (AD) was discovered by Akedo, and since then, this method has been used for various types of ceramic film fabrication [49][50][51][52][53]. The advantages of the AD method are the rapid ceramic film formation rate and the feasibility of room temperature impact consolidation (without heat treatment) [54][55]. To deposit composite ceramic films with good transparency and desired optical properties, a homogeneous mixture of starting materials is indispensable. Therefore, electrostatic assembled composite powder can be used to obtain the desired optical properties of aerosol-deposited ceramic films . With a homogeneous decoration of indium tin oxide (ITO) or cerium oxide (CeO_2) nanoparticles on Al_2O_3 as shown in Figure 9, tailoring of the ultraviolet and infrared light adsorption properties of transparent Al_2O_3 composite films have been recently reported. As shown in the schematics in Figure 9, inhomogeneous powder mixtures with agglomeration will affect the film deposition uniformity, thereby causing the property deterioration of the AD films as compared to electrostatically assembled composite powders.
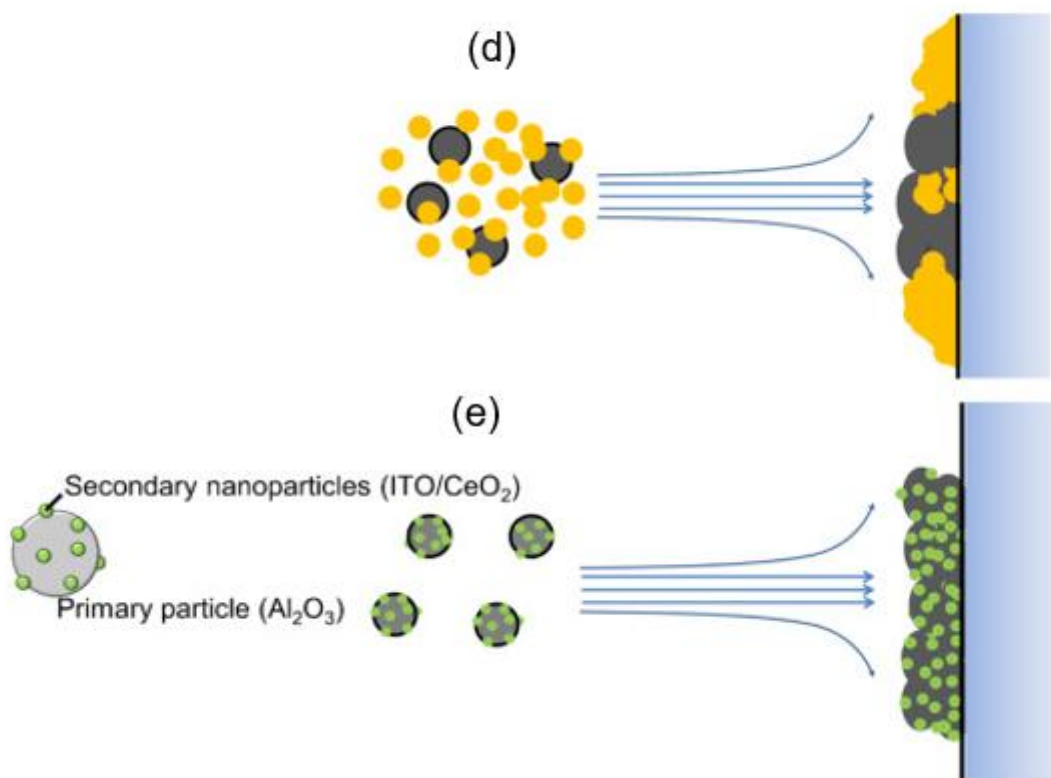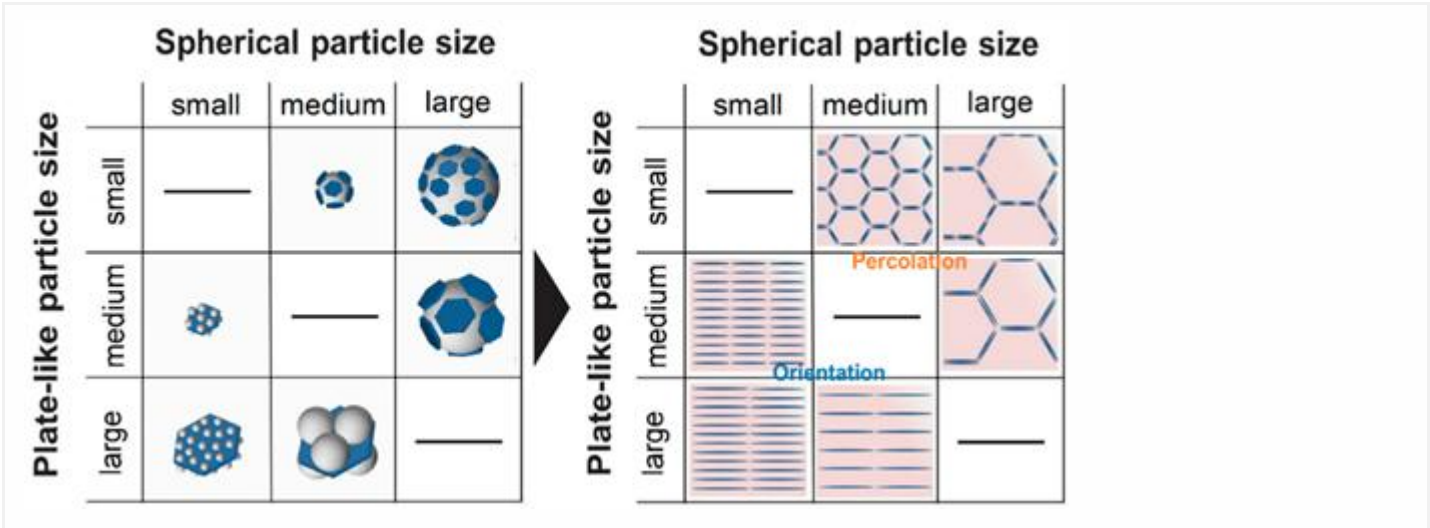
Figure 9. (**a**) Schematics of the ITO–Al_2O_3 and CeO_2–Al_2O_3 nanocomposite formation via an electrostatic adsorption method while (**b**,**c**) are the SEM images of the as-obtained ITO–Al_2O_3 and CeO_2–Al_2O_3 nanocomposites, respectively. The schematic of aerosol-deposited films using (**d**) mixed oxide nanoparticles and (**e**) homogenous electrostatically adsorbed nanocomposite oxide particles. Reprinted with permission from [31], copyright (2019) Elsevier.
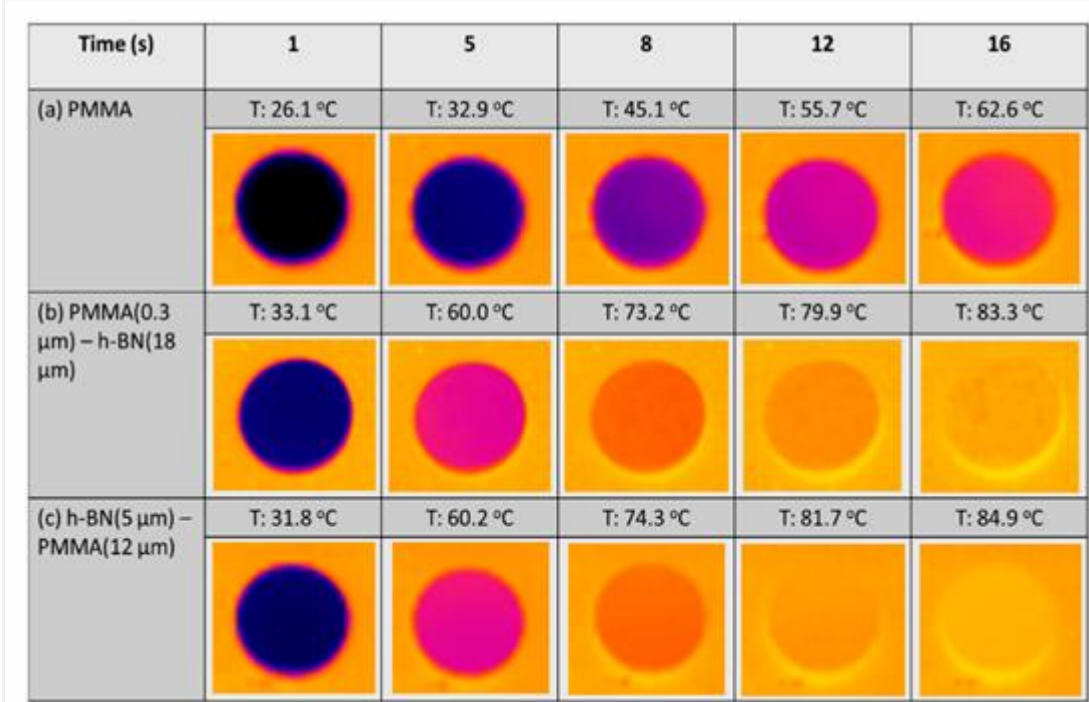
2.6. Controlled Properties of Poly (Methyl Methacrylate) (PMMA) Composites

In the design of lightweight and portable devices, advanced polymer composites with desired properties such as good heat conduction, electrical conductivity, and controlled optical properties are indispensable. The fabrication of high-performance polymer composites by controlling the homogeneity and distribution of the organic and inorganic material composition is one of the important factors for achieving desired properties without compromising the mechanical properties . Among the polymeric matrix materials available, poly (methyl methacrylate) (PMMA) is a well-known material due to its good optical clarity, mechanical strength, and thermal stability; they are said to possess the potential to replace glass in various applications [56]. By using the EA method, the homogenous distribution of functional materials within the PMMA matrix has been reported to enable the generation of desired and unique properties in PMMA matrix composites [57][58][59]. In a recent study, Yokoi et al. demonstrated the controllability of the thermal conductivity of hexagonal boron nitride (hBN)/PMMA composites by either adjusting the sizes of the hBN sheets or the particle size of PMMA particles used in the EA process . Interestingly, the controlled decoration of hBN sheets within the PMMA matrix led to either the percolation of hBN or a layer-oriented

microstructure demonstrating the different heat conduction behaviors, as shown in Figure 10. On the other hand, in a different application of infra-red (IR) filtering, Tan et al. reported the homogeneous decoration of nano-sized ITO particles within the PMMA matrix in the fabrication of IR filtering PMMA–ITO composite pellets . Precise control of the amount and decoration of ITO within the PMMA matrix is a crucial factor in maintaining the visible light transmission within the composite [60][61]. A good distribution of ITO nanoparticles within the matrix would generate a 3D-ITO framework creating plasmonic responses as well as electric field coupling that results in the IR ray reflectivity for filtering effect generation [62][63][64].

(A)

(B)

Figure 10. (**A**) Schematic illustrations showing the composite morphologies of hexagonal boron nitride (hBN)/poly (methyl methacrylate) (hBN/PMMA) and PMMA/hBN composite particles with the corresponding microstructures obtained. (**B**) Thermograph images of (a) PMMA, (b) PMMA (0.3 μm)/hBN (18 μm), and (c) hBN (5 μm)/PMMA (12 μm) composite pellets after infrared thermography irradiation. Reprinted with permission from [8], copyright (2020) MDPI.

References

1. Tan, W.K.; Araki, Y.; Yokoi, A.; Kawamura, G.; Matsuda, A.; Muto, H. Micro- and Nano-assembly of Composite Particles by Electrostatic Adsorption. Nanoscale Research Letters 2019, 14, 297, doi:10.1186/s11671-019-3129-1.

2. Subramaniam, M.N.; Goh, P.S.; Lau, W.J.; Ismail, A.F. The Roles of Nanomaterials in Conventional and Emerging Technologies for Heavy Metal Removal: A State-of-the-Art Review. Nanomaterials (Basel) 2019, 9, doi:10.3390/nano9040625.

3. Ariga, K.; Nakanishi, T.; Hill, J.P. Self-assembled microstructures of functional molecules. Current Opinion in Colloid & Interface Science 2007, 12, 106-120, doi:10.1016/j.cocis.2007.05.008.

4. Caruso, F.; Lichtenfeld, H.; Giersig, M.; Möhwald, H. Electrostatic Self-Assembly of Silica Nanoparticle−Polyelectrolyte Multilayers on Polystyrene Latex Particles. Journal of the American Chemical Society 1998, 120, 8523-8524, doi:10.1021/ja9815024.

5. Wu, C.; Aslan, S.; Gand, A.; Wolenski, J.S.; Pauthe, E.; Van Tassel, P.R. Porous Nanofilm Biomaterials Via Templated Layer-by-Layer Assembly. Advanced Functional Materials 2013, 23, 66-74, doi:10.1002/adfm.201201042.

6. Ariga, K.; Lvov, Y.M.; Kawakami, K.; Ji, Q.; Hill, J.P. Layer-by-layer self-assembled shells for drug delivery. Adv Drug Deliv Rev 2011, 63, 762-771, doi:10.1016/j.addr.2011.03.016.

7. Ariga, K.; Malgras, V.; Ji, Q.; Zakaria, M.B.; Yamauchi, Y. Coordination nanoarchitectonics at interfaces between supramolecular and materials chemistry. Coordination Chemistry Reviews 2016, 320-321, 139-152, doi:10.1016/j.ccr.2016.01.015.

8. Yokoi, A.; Tan, W.K.; Kuroda, T.; Kawamura, G.; Matsuda, A.; Muto, H. Design of Heat-Conductive hBN–PMMA Composites by Electrostatic Nano-Assembly. Nanomaterials 2020, 10, 134.

9. Tan, W.K.; Yokoi, A.; Kawamura, G.; Matsuda, A.; Muto, H. PMMA-ITO Composite Formation via Electrostatic Assembly Method for Infra-Red Filtering. Nanomaterials 2019, 9, doi:10.3390/nano9060886.

10. Tan, W.K.; Tsuzuki, K.; Yokoi, A.; Kawamura, G.; Matsuda, A.; Muto, H. Formation of porous Al2O3–SiO2 composite ceramics by electrostatic assembly. Journal of the Ceramic Society of Japan 2020, 128, 605-610, doi:10.2109/jcersj2.20064.

11. Fenoy, G.E.; Van der Schueren, B.; Scotto, J.; Boulmedais, F.; Ceolín, M.R.; Bégin-Colin, S.; Bégin, D.; Marmisollé, W.A.; Azzaroni, O. Layer-by-layer assembly of iron oxide-decorated few-layer graphene/PANI:PSS composite films for high performance supercapacitors operating in neutral aqueous electrolytes. Electrochimica Acta 2018, 283, 1178-1187, doi:10.1016/j.electacta.2018.07.085.

12. Zhang, X.; Chen, H.; Zhang, H. Layer-by-layer assembly: from conventional to unconventional methods. Chem Commun (Camb) 2007, 10.1039/b615590a, 1395-1405, doi:10.1039/b615590a.

13. Decher, G.; Hong, J.D.; Schmitt, J. Buildup of ultrathin multilayer films by a self-assembly process: III. Consecutively alternating adsorption of anionic and cationic polyelectrolytes on charged surfaces. Thin Solid Films 1992, 210-211, 831-835, doi:https://doi.org/10.1016/0040-6090(92)90417-A.

14. Decher, G. Fuzzy Nanoassemblies: Toward Layered Polymeric Multicomposites. Science 1997, 277, 1232-1237, doi:10.1126/science.277.5330.1232.

15. Rydzek, G.; Ji, Q.; Li, M.; Schaaf, P.; Hill, J.P.; Boulmedais, F.; Ariga, K. Electrochemical nanoarchitectonics and layer-by-layer assembly: From basics to future. Nano Today 2015, 10, 138-167, doi:10.1016/j.nantod.2015.02.008.

16. Boudou, T.; Crouzier, T.; Ren, K.; Blin, G.; Picart, C. Multiple functionalities of polyelectrolyte multilayer films: new biomedical applications. Adv Mater 2010, 22, 441-467, doi:10.1002/adma.200901327.

17. Ren, K.-f.; Hu, M.; Zhang, H.; Li, B.-c.; Lei, W.-x.; Chen, J.-y.; Chang, H.; Wang, L.-m.; Ji, J. Layer-by-layer assembly as a robust method to construct extracellular matrix mimic surfaces to modulate cell behavior. Progress in Polymer Science 2019, 92, 1-34, doi:10.1016/j.progpolymsci.2019.02.004.

18. Wang, F.; Wang, J.; Zhai, Y.; Li, G.; Li, D.; Dong, S. Layer-by-layer assembly of biologically inert inorganic ions/DNA multilayer films for tunable DNA release by chelation. J Control Release 2008, 132, 65-73, doi:10.1016/j.jconrel.2008.08.016.

19. Qi, Y.; Qin, K.; Zou, Y.; Lin, L.; Jian, Z.; Chen, W. Flexible electrochromic thin films with ultrafast response based on exfoliated V2O5 nanosheets/graphene oxide via layer-by-layer assembly. Applied Surface Science 2020, 514, doi:10.1016/j.apsusc.2020.145950.

20. Liu, X.Q.; Fourel, L.; Dalonneau, F.; Sadir, R.; Leal, S.; Lortat-Jacob, H.; Weidenhaupt, M.; Albiges-Rizo, C.; Picart, C. Biomaterial-enabled delivery of SDF-1alpha at the ventral side of

breast cancer cells reveals a crosstalk between cell receptors to promote the invasive phenotype. Biomaterials 2017, 127, 61-74, doi:10.1016/j.biomaterials.2017.02.035.

21. Kumar, R.; Sahoo, S.; Joanni, E.; Singh, R.K.; Tan, W.K.; Kar, K.K.; Matsuda, A. Recent progress in the synthesis of graphene and derived materials for next generation electrodes of high performance lithium ion batteries. Progress in Energy and Combustion Science 2019, 75, 100786, doi:https://doi.org/10.1016/j.pecs.2019.100786.

22. Phuc, N.H.H.; Takaki, M.; Muto, H.; Reiko, M.; Kazuhiro, H.; Matsuda, A. Sulfur–Carbon Nano Fiber Composite Solid Electrolyte for All-Solid-State Li–S Batteries. ACS Applied Energy Materials 2020, 3, 1569-1573, doi:10.1021/acsaem.9b02062.

23. Tan, W.K.; Matsuzaki, T.; Yokoi, A.; Kawamura, G.; Matsuda, A.; Muto, H. Improved green body strength using PMMA–Al2O3 composite particles fabricated via electrostatic assembly. Nano Express 2020.

24. Tan, W.K.; Asami, K.; Maeda, Y.; Hayashi, K.; Kawamura, G.; Muto, H.; Matsuda, A. Facile formation of Fe3O4-particles decorated carbon paper and its application for all-solid-state rechargeable Fe-air battery. Applied Surface Science 2019, 486, 257-264, doi:10.1016/j.apsusc.2019.04.278.

25. Kumar, R.; Sahoo, S.; Joanni, E.; Singh, R.K.; Maegawa, K.; Tan, W.K.; Kawamura, G.; Kar, K.K.; Matsuda, A. Heteroatom doped graphene engineering for energy storage and conversion. Materials Today 2020, 10.1016/j.mattod.2020.04.010, doi:10.1016/j.mattod.2020.04.010.

26. Hong, X.; Zhang, B.; Murphy, E.; Zou, J.; Kim, F. Three-dimensional reduced graphene oxide/polyaniline nanocomposite film prepared by diffusion driven layer-by-layer assembly for high-performance supercapacitors. Journal of Power Sources 2017, 343, 60-66, doi:10.1016/j.jpowsour.2017.01.034.

27. Nbelayim, P.; Ashida, Y.; Maegawa, K.; Kawamura, G.; Muto, H.; Matsuda, A. Preparation and Characterization of Stable and Active Pt@TiO2 Core–Shell Nanoparticles as Electrocatalyst for Application in PEMFCs. ACS Applied Energy Materials 2020, 3, 3269-3281, doi:10.1021/acsaem.9b02169.

28. Che, Q.; Fan, H.; Duan, X.; Feng, F.; Mao, W.; Han, X. Layer by layer self-assembly fabrication of high temperature proton exchange membrane based on ionic liquids and polymers. Journal of Molecular Liquids 2018, 269, 666-674, doi:10.1016/j.molliq.2018.08.030.

29. Ooi, Y.X.; Ya, K.Z.; Maegawa, K.; Tan, W.K.; Kawamura, G.; Muto, H.; Matsuda, A. CHS-WSiA doped hexafluoropropylidene-containing polybenzimidazole composite membranes for medium temperature dry fuel cells. International Journal of Hydrogen Energy 2019, 44, 32201-32209, doi:10.1016/j.ijhydene.2019.10.093.

30. Ooi, Y.X.; Ya, K.Z.; Maegawa, K.; Tan, W.K.; Kawamura, G.; Muto, H.; Matsuda, A. Incorporation of titanium pyrophosphate in polybenzimidazole membrane for medium temperature dry PEFC application. Solid State Ionics 2020, 344, doi:10.1016/j.ssi.2019.115140.

31. Maegawa, K.; Zay Ya, K.; Tan, W.K.; Kawamura, G.; Hattori, T.; Muto, H.; Matsuda, A. Enhancement of interfacial property by novel solid ionomer CsHSO4-H4SiW12O40 for the three-phase interface of a medium-temperature anhydrous fuel cell. Materials Letters 2019, 253, 201-204, doi:10.1016/j.matlet.2019.06.061.

32. Meemuk, C.; Chirachanchai, S. Constructing polymeric proton donor and proton acceptor in layer-by-layer structure for efficient proton transfer in PEMFC. International Journal of Hydrogen Energy 2016, 41, 4765-4772, doi:10.1016/j.ijhydene.2016.01.069.

33. Ibbett, J.; Tafazzolimoghaddam, B.; Hernandez Delgadillo, H.; Curiel-Sosa, J.L. What triggers a microcrack in printed engineering parts produced by selective laser sintering on the first place? Materials & Design 2015, 88, 588-597, doi:10.1016/j.matdes.2015.09.026.

34. Sofia, D.; Barletta, D.; Poletto, M. Laser sintering process of ceramic powders: The effect of particle size on the mechanical properties of sintered layers. Additive Manufacturing 2018, 23, 215-224, doi:10.1016/j.addma.2018.08.012.

35. Tofail, S.A.M.; Koumoulos, E.P.; Bandyopadhyay, A.; Bose, S.; O'Donoghue, L.; Charitidis, C. Additive manufacturing: scientific and technological challenges, market uptake and opportunities. Materials Today 2018, 21, 22-37, doi:10.1016/j.mattod.2017.07.001.

36. Chen, Z.; Li, Z.; Li, J.; Liu, C.; Lao, C.; Fu, Y.; Liu, C.; Li, Y.; Wang, P.; He, Y. 3D printing of ceramics: A review. Journal of the European Ceramic Society 2019, 39, 661-687, doi:10.1016/j.jeurceramsoc.2018.11.013.

37. Hwa, L.C.; Rajoo, S.; Noor, A.M.; Ahmad, N.; Uday, M.B. Recent advances in 3D printing of porous ceramics: A review. Current Opinion in Solid State and Materials Science 2017, 21, 323-347, doi:10.1016/j.cossms.2017.08.002.

38. Lee, J.-Y.; An, J.; Chua, C.K. Fundamentals and applications of 3D printing for novel materials. Applied Materials Today 2017, 7, 120-133, doi:10.1016/j.apmt.2017.02.004.

39. Amin Yavari, S.; Croes, M.; Akhavan, B.; Jahanmard, F.; Eigenhuis, C.C.; Dadbakhsh, S.; Vogely, H.C.; Bilek, M.M.; Fluit, A.C.; Boel, C.H.E., et al. Layer by layer coating for bio-functionalization of additively manufactured meta-biomaterials. Additive Manufacturing 2020, 32, doi:10.1016/j.addma.2019.100991.

40. Shin, J.-H.; Choi, J.; Kim, M.; Hong, S.-H. Comparative study on carbon nanotube- and reduced graphene oxide-reinforced alumina ceramic composites. Ceramics International 2018, 44, 8350-8357, doi:10.1016/j.ceramint.2018.02.024.

41. Zhan, G.-D.; Kuntz, J.D.; Wan, J.; Mukherjee, A.K. Single-wall carbon nanotubes as attractive toughening agents in alumina-based nanocomposites. Nature Materials 2002, 2, 38, doi:10.1038/nmat793.

42. Kumari, L.; Zhang, T.; Du, G.; Li, W.; Wang, Q.; Datye, A.; Wu, K. Thermal properties of CNT-Alumina nanocomposites. Composites Science and Technology 2008, 68, 2178-2183, doi:10.1016/j.compscitech.2008.04.001.

43. Dionigi, C.; Ivanovska, T.; Ortolani, L.; Morandi, V.; Ruani, G. Electrically conductive gamma-alumina/amorphous carbon nano-composite foams. Journal of Alloys and Compounds 2017, 694, 921-928, doi:10.1016/j.jallcom.2016.10.056.

44. Petit, C.; Montanaro, L.; Palmero, P. Functionally graded ceramics for biomedical application: Concept, manufacturing, and properties. International Journal of Applied Ceramic Technology 2018, 15, 820-840, doi:10.1111/ijac.12878.

45. Meille, S.; Lombardi, M.; Chevalier, J.; Montanaro, L. Mechanical properties of porous ceramics in compression: On the transition between elastic, brittle, and cellular behavior. Journal of the European Ceramic Society 2012, 32, 3959-3967, doi:10.1016/j.jeurceramsoc.2012.05.006.

46. Ali, M.S.; Hanim, M.A.A.; Tahir, S.M.; Jaafar, C.N.A.; Norkhairunnisa, M.; Matori, K.A. Preparation and characterization of porous alumina ceramics using different pore agents. Journal of the Ceramic Society of Japan 2017, 125, 402-412, doi:10.2109/jcersj2.16233.

47. Ohji, T.; Fukushima, M. Macro-porous ceramics: processing and properties. International Materials Reviews 2012, 57, 115-131, doi:10.1179/1743280411Y.0000000006.

48. Akedo, J. Room Temperature Impact Consolidation (RTIC) of Fine Ceramic Powder by Aerosol Deposition Method and Applications to Microdevices. Journal of Thermal Spray Technology 2008, 17, 181-198, doi:10.1007/s11666-008-9163-7.

49. Akedo, J. Room temperature impact consolidation and application to ceramic coatings: aerosol deposition method. Journal of the Ceramic Society of Japan 2020, 128, 101-116, doi:10.2109/jcersj2.19196.

50. Adamczyk, J.; Fuierer, P. Compressive stress in nano-crystalline titanium dioxide films by aerosol deposition. Surface and Coatings Technology 2018, 350, 542-549, doi:10.1016/j.surfcoat.2018.07.015.

51. Cho, M.-Y.; Park, S.-J.; Kim, S.-M.; Lee, D.-W.; Kim, H.-K.; Koo, S.-M.; Moon, K.-S.; Oh, J.-M. Hydrophobicity and transparency of Al 2 O 3 -based poly-tetra-fluoro-ethylene composite thin films using aerosol deposition. Ceramics International 2018, 44, 16548-16555, doi:10.1016/j.ceramint.2018.06.076.

52. Exner, J.; Schubert, M.; Hanft, D.; Stöcker, T.; Fuierer, P.; Moos, R. Tuning of the electrical conductivity of Sr(Ti,Fe)O 3 oxygen sensing films by aerosol co-deposition with Al 2 O 3. Sensors

and Actuators B: Chemical 2016, 230, 427-433, doi:10.1016/j.snb.2016.02.033.

53. Hahn, B.-D.; Lee, J.-M.; Park, D.-S.; Choi, J.-J.; Ryu, J.; Yoon, W.-H.; Lee, B.-K.; Shin, D.-S.; Kim, H.-E. Aerosol deposition of silicon-substituted hydroxyapatite coatings for biomedical applications. Thin Solid Films 2010, 518, 2194-2199, doi:10.1016/j.tsf.2009.09.024.

54. Akedo, J. Aerosol Deposition of Ceramic Thick Films at Room Temperature: Densification Mechanism of Ceramic Layers. Journal of the American Ceramic Society 2006, 89, 1834-1839, doi:10.1111/j.1551-2916.2006.01030.x.

55. Akedo, J.; Nakano, S.; Park, J.; Baba, S.; Ashida, K. The aerosol deposition method; For production of high performance micro devices with low cost and low energy consumption. Synthesiology English edition 2008, 1, 121-130, doi:10.5571/syntheng.1.121.

56. Cierech, M.; Osica, I.; Kolenda, A.; Wojnarowicz, J.; Szmigiel, D.; Lojkowski, W.; Kurzydlowski, K.; Ariga, K.; Mierzwinska-Nastalska, E. Mechanical and Physicochemical Properties of Newly Formed ZnO-PMMA Nanocomposites for Denture Bases. Nanomaterials (Basel) 2018, 8, doi:10.3390/nano8050305.

57. Arul, K.T.; Ramanjaneyulu, M.; Ramachandra Rao, M.S. Energy harvesting of PZT/PMMA composite flexible films. Current Applied Physics 2019, 19, 375-380, doi:10.1016/j.cap.2019.01.003.

58. Nayak, D.; Choudhary, R.B. Augmented optical and electrical properties of PMMA-ZnS nanocomposites as emissive layer for OLED applications. Optical Materials 2019, 91, 470-481, doi:10.1016/j.optmat.2019.03.040.

59. Sugumaran, S.; Bellan, C.S. Transparent nano composite PVA–TiO2 and PMMA–TiO2 thin films: Optical and dielectric properties. Optik 2014, 125, 5128-5133, doi:10.1016/j.ijleo.2014.04.077.

60. Arlindo, E.P.S.; Lucindo, J.A.; Bastos, C.M.O.; Emmel, P.D.; Orlandi, M.O. Electrical and Optical Properties of Conductive and Transparent ITO@PMMA Nanocomposites. The Journal of Physical Chemistry C 2012, 116, 12946-12952, doi:10.1021/jp3031418.

61. Arlindo, E.P.S.; Orlandi, M.O. Study ITO@PMMA Composites by Transmission Electron Microscopy. MRS Proceedings 2011, 1312, doi:10.1557/opl.2011.217.

62. Matsui, H.; Furuta, S.; Hasebe, T.; Tabata, H. Plasmonic-Field Interactions at Nanoparticle Interfaces for Infrared Thermal-Shielding Applications Based on Transparent Oxide Semiconductors. ACS Applied Materials & Interfaces 2016, 8, 11749-11757, doi:10.1021/acsami.6b01202.

63. Matsui, H.; Tabata, H. Assembled Films of Sn-Doped In2O3 Plasmonic Nanoparticles on High-Permittivity Substrates for Thermal Shielding. ACS Applied Nano Materials 2019, 2, 2806-2816, doi:10.1021/acsanm.9b00293.

64. Matsui, H.; Tabata, H. Infrared Solar Thermal-Shielding Applications Based on Oxide Semiconductor Plasmonics. In Nanoplasmonics - Fundamentals and Applications, 2017; 10.5772/67588.

65. Matsui, H.; Tabata, H. Infrared Solar Thermal-Shielding Applications Based on Oxide Semiconductor Plasmonics. In Nanoplasmonics - Fundamentals and Applications, 2017; 10.5772/67588.

Retrieved from https://encyclopedia.pub/entry/history/show/9465